

# Deformable 1D Photonic Crystal Nanolasers for Planar Strain Identification

Tsan-Wen Lu\*, Chia-Cheng Wu, and Po-Tsung Lee

Department of Photonics, National Chiao Tung Univ.  
Rm. 401 CPT Building, 1001 Ta-Hsueh Road, Hsinchu 30010, Taiwan  
Phone: +886-3-5712121 ext. 59341, E-mail: tsanwenlu@gmail.com

## Abstract

1D photonic crystal nanolaser wrapped by a deformable polydimethylsiloxane is demonstrated with wide wavelength tunable range. By studying its wavelength response to non-axial deformations both in experiments and simulations, a novel strain sensor with capability of identifying the applied planar strain direction, type, and strength can be expected.

## 1. Introduction

Photonic crystals (PhCs) have long been regarded as a good platform to realize various efficient nano-photonic devices in hard and soft photonic integrated circuits (PICs). In recent years, owing to the rapid developments of wearable devices and systems, PhC devices have also been utilized in strain sensing by the optical responses to different lattice deformations in literatures [1-3]. However, most of them are realized by 2D PhCs, which possess disadvantages of large layout footprints in PICs and/or low sensitivity caused by continuous lattice structures. In our previous work, we have demonstrated a discontinuous 1D PhC nanoblocks laser [4] with small device footprint and large wavelength response to the applied stretching. Unfortunately, all these

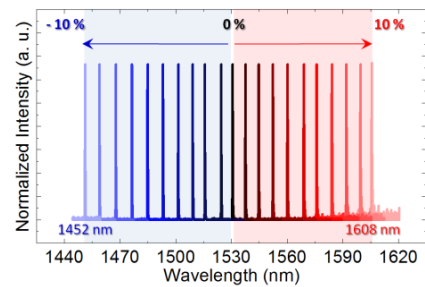


Fig. 2 Lasing spectra of the single nanolaser under 10% compression to 10% stretching.

reports assume that the applied strain direction is known in advance, which means they actually cannot identify an unknown planar strain when serving as a strain sensor. In this report, a novel strain sensor based on deformable 1D PhC nanolasers with capability of identifying the direction, type, and strength of planar strain is proposed.

## 2. Design & Experimental Results

Schematic of our proposed nanolaser shown in Fig. 1(a) is consisted of 1D periodic nanorods (PhCs) wrapped by a deformable polydimethylsiloxane (PDMS). The lattice constant ( $a$ ), width ( $w$ ), and length ( $L$ ) of 1D PhCs are all defined in the inset of Fig. 1(a). To locally confine the first photonic band within this structure,  $w$  and  $a$  both linearly increase by 10-nm increments from the center to the edges of the PhCs to form a mode-gap confined nanocavity, as shown by the top- and magnified tilted-view SEM images in Fig. 1(b). The nanocavity before embedding into PDMS in Fig. 1(b) is manufactured by a series of lithography and etching processes, which is followed by embedding into a PDMS substrate using transferring techniques [4]. Figure 1(c) shows the images of PDMS substrate with PhC devices array under compression and optical microscope. Figure 1(d) shows the theoretical  $|E|$  field of the first band confined in this nanocavity by 3D finite-element method. The sufficiently high quality factor ( $Q$ ) of 6,700 and a small mode volume of  $1.25(\lambda/n)^3$  show its capability for lasing.

In measurements, single mode lasing near wavelength of 1530 nm is obtained from the device under a laser pulse pumping with 15 ns width at room temperature, as shown in Fig. 2. By further applying compression from 0 to 10% and stretching from 0 to 10% to the PDMS substrate, a very wide wavelength tunable range of 156 nm (from 1452 to 1608 nm, almost spans the entire S+C+L band) is successfully demonstrated with a single nanolaser device, as shown

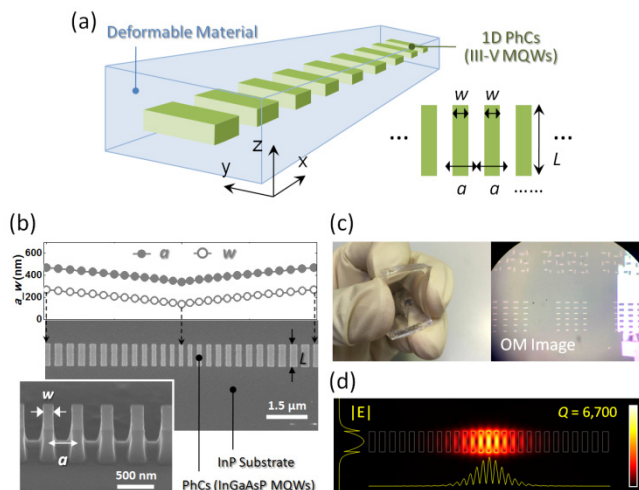


Fig. 1 (a) Schematic and parameters of 1D PhCs wrapped by PDMS. (b) (top) Spatial distributions of  $a$  and  $w$  of the PhC nanocavity and (bottom) the top- and magnified tilted-view SEM images before embedding into PDMS. (c) Images of PDMS substrate with PhC devices array under (left) compression and (right) optical microscope. (d) Theoretical mode profile in  $|E|$  field of the confined dielectric mode in the nanocavity along the  $xy$ -plane.

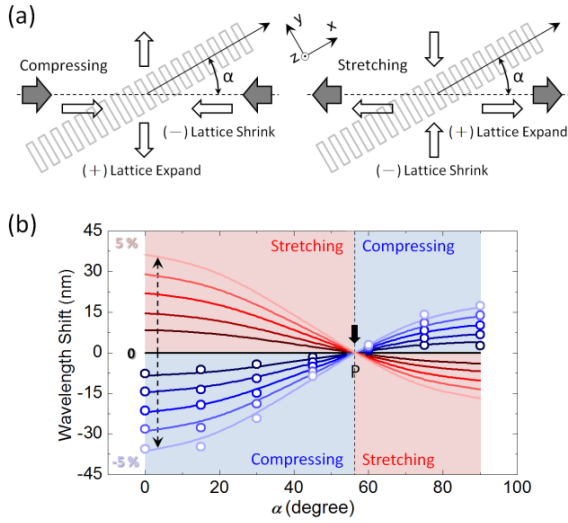


Fig. 3 (a) Schematics of lattice deformations of 1D PhC nanolaser caused by non-axial (left) compression and (right) stretching. (b) Theoretical wavelength shifts of devices with different  $\alpha$  under different stretching and compressing from 0 to 5%.

in Fig. 2. This results in a high wavelength tunability of 7.8 nm under 1% deformation, which agrees with our previous results and the conclusion of its strain sensing capability [4].

So far, the applied strains (stretching/compression) are all along the periodic direction ( $x$ -axis) of 1D PhCs. Figure 3(a) shows the schematics of lattice deformations of the nanolaser under the compression and stretching orientated to PhC periodic direction by an angle of  $\alpha$ . In Fig. 3(a), the compressive strain applied to the device will give rise to a stretching orthogonal to the strain applying direction simultaneously because of positive Poisson ratio ( $\sim 0.495$ ) of the PDMS. That is, when  $0^\circ < \alpha < 90^\circ$ , the nanolaser will show wavelength shift composed of the lattice decreasing (blue-shift) and increasing (red-shift) by the compressive strain and a resultant stretching strain along the orthogonal direction. When  $\alpha = 0^\circ$ , the lattice decrement (blue-shift) is totally contributed by the applied compressive strain. In contrast, when  $\alpha = 90^\circ$ , the resultant stretching orthogonal to the strain applying direction is responsible for the lattice increment (red-shift). Figure 3(b) shows theoretical wavelength shifts of the nanolasers with different  $\alpha$  under different stretching and compression from 0 to 5%. It is worthy to note that all the curves intersect at the point  $P$  ( $\alpha \sim 57^\circ$ ), where the wavelength shifts that come from compressing and resultant stretching are equal and the nanolaser shows no response to the applied strain.

To verify above properties, we propose and demonstrate a layout design consisted of 1D PhC nanolasers  $A$  to  $G$  arranged with  $\alpha$  from  $0^\circ$  to  $90^\circ$  by  $15^\circ$  increment, as shown by the inset SEM image in Fig. 4. In measurements, we apply a compressive strain from 0 to 5% (1% increment) along  $x$ -axis to these devices, whose lasing spectra are shown in Fig. 4. Taking 5% compression for example, the wavelength shift ( $\Delta\lambda_{-5\%}$ ) for device  $A$  shows a blue-shift of

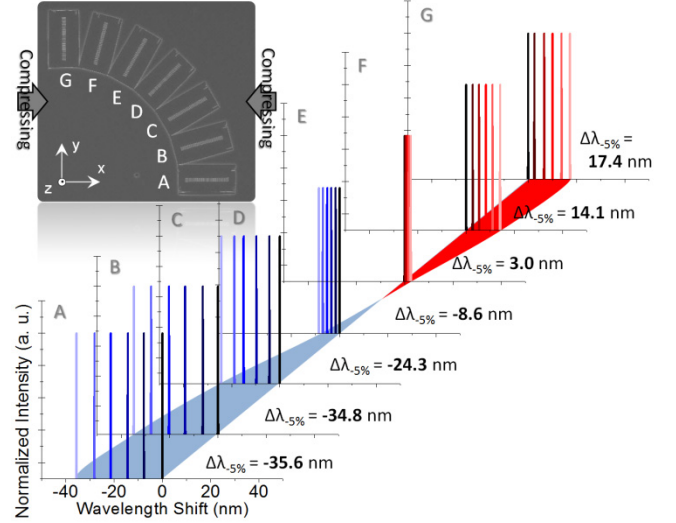


Fig. 4 Lasing spectra from the devices with different  $\alpha$  from  $0^\circ$  to  $90^\circ$  (devices  $A$ - $G$ , as shown by the inset SEM image) under different compressions from 0 to 5%.

-35.6 nm, while it shows gradually decreased blue-shifts for devices  $B$ ,  $C$ , and  $D$ . For device  $E$ , the  $\Delta\lambda_{-5\%}$  becomes a red-shift of 3 nm, where the resultant stretching along  $y$ -axis dominates the wavelength shift. For device  $G$ ,  $\Delta\lambda_{-5\%}$  shows red-shift of 17.4 nm, which completely comes from the resultant stretching along  $y$ -axis. The recorded  $\Delta\lambda_{-5\%}$  of nanolasers with different  $\alpha$  denoted by open circles in Fig. 3(b), as well as those under different compressions, all agree with the simulation results very well.

Therefore, the results shown in Fig. 3(b) could be a database for the layout design shown in Fig. 4 in strain sensing. Via fitting the measured wavelength shifts from the devices  $A$  to  $G$  under an unknown arbitrary planar strain with the curves in Fig. 3(b), the direction, type, and strength of the applied strain can be easily estimated.

### 3. Conclusions

We have demonstrated a 1D PhC nanolaser buried in a deformable PDMS with wide wavelength tunable range of 156 nm. We further studied the wavelength response of this device to non-axial deformations both in experiments and simulations. These results can be served as a database for our proposed layout design, which enables a novel sensor with capability of identifying an unknown planar strain, including its direction, type, and strength.

### References

- [1] B. T. Tung, D. V. Dao, T. Ikeda, Y. Kanamori, K. Hane, and S. Sugiyama, *Opt. Express* **19** (2011) 8821.
- [2] T. Karrock and M. Gerken, *Biomed. Opt. Express* **6** (2015) 4901.
- [3] J. H. Choi, Y. S. No, J. P. So, J. M. Lee, K. H. Kim, M. S. Hwang, S. H. Kwon, and H. G. Park, *Nat. Comm.* **7** (2016) 11569.
- [4] T. W. Lu, C. Wang, C. F. Hsiao, and P. T. Lee, *Nanoscale* **8** (2016) 16769.